NATIONAL ADVISORY COMMITTEE FOR AERONAUTICS

TECHNICAL NOTE 2566

A STUDY OF ELASTIC AND PLASTIC STRESS CONCENTRATION FACTORS DUE TO NOTCHES AND FILLETS IN FLAT PLATES

By Herbert F. Hardrath and Lachlan Ohman

Langley Aeronautical Laboratory
Langley Field, Va.

Washington
December 1951

NATIONAL ADVISORY COMMITTEE FOR AERONAUTICS

TECHNICAL NOTE 2566

A STUDY OF ELASTIC AND PLASTIC STRESS CONCENTRATION FACTORS DUE TO NOTCHES AND FILLETS IN FLAT PLATES

By Herbert F. Hardrath and Lachlan Ohman

SUMMARY

Six large 24S-T3 aluminum-alloy-sheet specimens containing various notches or fillets were tested in tension to determine their stress concentration factors in both the elastic and plastic ranges.

The elastic stress concentration factors were found to be slightly higher than those calculated by Neuber's method and those obtained photoelastically by Frocht. The results showed further that the stress concentration factor decreases as strains at the discontinuity enter the plastic range.

A generalization of Stowell's relation for the plastic stress concentration factor at a circular hole in an infinite plate was applied to the specimen shapes tested and gave good agreement with test results.

INTRODUCTION

Theoretical studies of stress concentrations around discontinuities in flat plates have been limited because of analytical difficulties to certain geometric shapes (references 1 to 6) and, until recently, to the realm of stresses in the elastic range. Experimental studies on the subject are scarce, such investigations being limited by available loading and strain measuring equipment (references 7 to 11). The present investigation was undertaken to obtain experimentally stress concentration data in both the elastic and plastic ranges for sheet specimens containing a variety of notches and fillets.

A formula has been presented by Stowell (reference 12) for the stress concentration factor in the plastic range for a circular hole in an infinite plate. When the formula is written in a generalized form it appears to be applicable to the specimen shapes of this investigation and to other configurations.

EXPERIMENTAL PROCEDURE

Since the maximum stress in a panel containing a stress concentration occurs at a point and the stress distribution around the point follows a gradient, it is essential for reliable measurements that the ratio of notch dimensions to gage length of the strain gages be as large as possible. Therefore, in order to obtain a high ratio and to be able to use strain gages of practical dimensions, the specimens were made 48 by 142 inches.

The specimens consisted of six 24S-T3 aluminum-alloy panels $\frac{1}{8}$ inch thick. Three panels, designated herein by N, contained notches; three, designated by F, contained fillets. In each group of three there was a panel designed to have a nominal stress concentration factor of 2, one of 4, and one of 6; hence the specimens are designated N2, N4, N6 and F2, F4, and F6. (Specimen dimensions are shown in detail in figs. 1 and 2.)

The panels were cut from sheets 54 inches wide. Excess material from the region near the notches or fillets was used to make standard tensile coupons, four for each panel. Standard tensile tests run on these coupons yielded stress-strain curves. Each of the stress-strain curves as presented in figure 3 is an average of the four curves obtained from the four coupons for each panel.

Four types of strain gages were used in the investigation. On panels N2 and F2 Tuckerman optical strain gages with a $\frac{1}{4}$-inch gage length were mounted on the face at the edge of the panel at the critical points which are defined as the points on each panel where the maximum stress concentrations occur. In a notched specimen the maximum stress occurs at the center of the base of the notch. Photoelastic studies of filleted specimens (reference 6) indicate that the maximum stress occurs at a point about 10° around the fillet from the tangent between the fillet and the straight side of the reduced part of the panel. Strains at the critical points of panels N4, N6, F4, and F6 were measured with $\frac{1}{16}$-inch-gage-length electromagnetic extensometers mounted on the edges of the panels at the critical points. (See figs. 1 and 2.)

Baldwin SR-4 type A-5 strain gages were applied at intervals across the width of each panel at the net section to determine the strain distribution at that section (figs. 1 and 2). In a notched panel the net section is defined as the cross section through the panel between the two critical points (fig. 1). In a filleted panel the net section is defined as the section across the panel containing the points where

the fillets and the straight sides of the reduced part of the panel are tangent (fig. 2). Baldwin SR-4 type A-1 strain gages were applied at other cross sections (figs. 1 and 2) to ascertain the uniformity of load application.

Load and strain readings were taken throughout each test at successive increments from zero load to a load which produced approximately 2 percent strain at the critical point.

RESULTS AND DISCUSSION

Elastic Stress Concentration Factors

The stress concentration factor is defined in this paper as the ratio of the stress at the critical point σ_{cp} to the average net section stress σ_{av}. The elastic stress concentration factor $K_{elastic}$ is computed from measurements taken before plastic yielding occurred in the specimen. The value of $K_{elastic}$ thus obtained for each specimen is presented in the second column of the table which follows:

Panel	$K_{elastic}$ (Experimental)	$K_{elastic}$ (Calculated by Neuber's Method)	$K_{elastic}$ (Determined photoelastically by Frocht)
N2	2.08	2.00	2.02
N4	4.26	4.00	4.02
N6	6.41	6.00	6.00
F2	1.88	....	....
F4	3.87	....	3.49
F6	5.44	....	5.00

The third column of the table lists the elastic stress concentration factors for the notched specimens as calculated by an analytical method presented by Neuber (reference 1) who, for reasons of mathematical convenience, treated notches with a hyperbolic contour. The computed value of the stress concentration factor in each case is based on a hyperbolic notch that has its depth and minimum radius of curvature equal to the depth and radius of the corresponding experimental notch. The experimental notch contour rather than being hyperbolic, however, is composed of a semicircular base with straight, parallel tangents, a

shape which is somewhat sharper than the corresponding hyperbolic notch. The experimental stress concentration factors, therefore, would be expected to be somewhat higher than those computed by Neuber's method. A comparison of values shown in the preceding table indicates the difference to be from 4 to 7 percent.

A photoelastic investigation of elastic stress concentration factors for shapes geometrically similar to those used in this investigation was performed by Frocht under the sponsorship of the National Advisory Committee for Aeronautics (reference 10). The results of this investigation are given in the fourth column of the preceding table. The results of the present investigation were found to be 4 to 7 percent higher for the notched specimens and 3 to 10 percent higher for the filleted specimens than the factors obtained photoelastically by Frocht. Although Frocht's values are nearly equal to those determined by Neuber's method, Frocht states that his values can be in error by as much as 10 percent for high stress concentration factors because of difficulties in determining the maximum fringe value near the boundary of sharp notches.

A comparison of elastic stress concentration factors determined by the three methods is given in figures 4 and 5.

Plastic Stress Concentration Factors and a Suggested Formula

Figures 6 and 7 show the experimentally determined stress concentration factors plotted against average net-section stress. The stress concentration factors start to decrease as the load on a panel exceeds a value sufficient to cause plastic yielding at the critical point.

Stowell (reference 12) presented a relation to be used in calculating the stress concentration factor in the plastic range for a circular hole in an infinite plate subjected to tension. This relation states that at any one instant in the loading

$$\frac{\sigma_{cp}}{\sigma_{\infty}} = 1 + 2\frac{E_S}{E_{\infty}} \qquad (1)$$

where

σ_{cp} stress occurring at the point of maximum stress

σ_{∞} average stress at points far removed from hole

E_S secant modulus of material at point of maximum stress

E_{∞} secant modulus of material at points far removed from hole

For the case when all stresses are elastic, the formula yields the value of 3, which is the theoretical elastic stress concentration factor for a circular hole in an infinite plate (reference 6). Predictions by formula (1) agreed well (reference 12) with the results of an experimental investigation reported by Griffith (reference 8) concerning the stress concentration factor for a circular hole in a flat sheet subjected to tension.

By rewriting formula (1) in a generalized form a relation between $K_{elastic}$ and $K_{plastic}$ may be obtained:

$$K_{plastic} = 1 + (K_{elastic} - 1)\frac{E_S}{E_\infty} \qquad (2)$$

where $K_{plastic}$ is the stress concentration factor in the plastic range. This form suggests that the formula might also be made applicable to shapes other than round holes by inserting a value for $K_{elastic}$ to correspond to the particular shape being considered. The plastic stress concentration factor for each of the specimens tested was computed by formula (2) with the experimental $K_{elastic}$ given in the preceding table, and the curves in figures 6 and 7 show that the generalized formula produced excellent agreement with the test results. A comparison between predictions by formula (2) and experimental results obtained by Box (reference 9) for other configurations is given in the appendix.

Strain and Stress Distributions

Strains measured by strain gages at four symmetrical locations on the net section of a panel were averaged to obtain the strain at a single station. These values are plotted for each of the six panels as the longitudinal strain distribution across half of the net section (parts "a", figs. 8 to 13).

The apparent stresses corresponding to strains at individual stations were obtained by using the stress-strain curves for the material (fig. 3) and are plotted for each panel as the longitudinal stress distribution across half the net section (parts "b", figs. 8 to 13). The apparent stresses so determined are not the true stresses at any stations other than those at the edges because stress conditions in the sheet are not uniaxial. The illustrated trends of the apparent stress distributions, however, are representative of the actual stress distributions.

CONCLUDING REMARKS

The elastic stress concentration factors were determined experimentally for six different specimens and were found to be 4 to 7 percent higher for the notched specimens and 3 to 10 percent higher for the filleted specimens than the factors obtained photoelastically by Frocht for shapes geometrically similar to those tested. The experimentally determined factors are 4 to 7 percent higher than those predicted for hyperbolic notches by Neuber's analytical method.

The stress concentration factors decreased as the strains at the critical points entered the plastic range and were found to agree well with calculated results obtained from the following equation which is a generalization of a relation originally presented by Stowell for the plastic stress concentration factor at a circular hole in an infinite plate:

$$K_{plastic} = 1 + (K_{elastic} - 1)\frac{E_S}{E_\infty}$$

where

$K_{plastic}$ stress concentration factor in plastic range

$K_{elastic}$ stress concentration factor in elastic range

E_S secant modulus of material at point of maximum stress

E_∞ secant modulus of material at points removed from hole

The generalized equation also checks well with experimental work done by Box on stress concentration factors in the plastic range for several additional configurations.

Langley Aeronautical Laboratory
National Advisory Committee for Aeronautics
Langley Field, Va., September 7, 1951

APPENDIX

COMPARISON OF SUGGESTED FORMULA WITH ADDITIONAL DATA

Additional experimental data on the effect of plasticity on the stress concentration factors for various configurations have been reported by Box (reference 9). Six flat sheet specimens were tested in tension: one contained semicircular notches, one had two holes symmetrically spaced in one cross section, one had a single hole elongated in the transverse direction, and three had single holes at various positions across the width of the specimens. The specimens, made of 24S-T3 aluminum alloy, were $4\frac{1}{2}$ inches wide, and the radius of all holes was 1/2 inch. The stress-strain curve for the material is reproduced as figure 14.

Comparisons of these data and predictions by formula (2) are presented in figures 15 to 20. Since the strain measuring technique employed by Box gave inaccurate results for small strains, but improved in accuracy for higher strains, the calculations were based on an experimental value of $K_{elastic}$ obtained near the high end of the elastic range. The resulting predictions of $K_{plastic}$ by formula (2) agree well with the experimental results obtained by Box.

REFERENCES

1. Neuber, Heinz: Theory of Notch Stresses: Principles for Exact Stress Calculation. J. W. Edwards (Ann Arbor, Mich.), 1946.

2. Sjöström, S.: On the Stresses at the Edge of an Eccentrically Located Circular Hole in a Strip under Tension. Rep. No. 36, Aero. Res. Inst. of Sweden (Stockholm), 1950.

3. Ling, Chih-Bing: Stresses in a Notched Strip under Tension. Jour. Appl. Mech., vol. 14, no. 4, Dec. 1947, pp. A-275 - A-280.

4. Ling, Chih-Bing: On the Stresses in a Plate Containing Two Circular Holes. Jour. Appl. Physics, vol. 19, no. 1, Jan. 1948, pp. 77-82.

5. Howland, R. C. J.: On the Stresses in the Neighborhood of a Circular Hole in a Strip Under Tension. Phil. Trans. Roy. Soc. (London), ser. A, vol. 229, Jan. 6, 1930.

6. Timoshenko, S.: Theory of Elasticity. First ed., McGraw-Hill Book Co., Inc., 1934.

7. Timoshenko, S.: Strength of Materials. Part II - Advanced Theory and Problems. Second ed., D. Van Nostrand Co., Inc., 1941.

8. Griffith, George E.: Experimental Investigation of the Effects of Plastic Flow in a Tension Panel with a Circular Hole. NACA TN 1705, 1948.

9. Box, William A.: The Effect of Plastic Strains on Stress Concentrators. Proc. Soc. Experimental Stress Analysis, vol. VIII, no. 2, 1951, pp. 99-110.

10. Frocht, M. M.: A Photoelastic Investigation of Stress Concentrations Due to Small Fillets and Grooves in Tension. NACA TN 2442, 1951.

11. Coker, E. G., and Filon, L. N. G.: A Treatise on Photo-Elasticity. Cambridge Univ. Press, (London) 1931.

12. Stowell, Elbridge Z.: Stress and Strain Concentration at a Circular Hole in an Infinite Plate. NACA TN 2073, 1950.

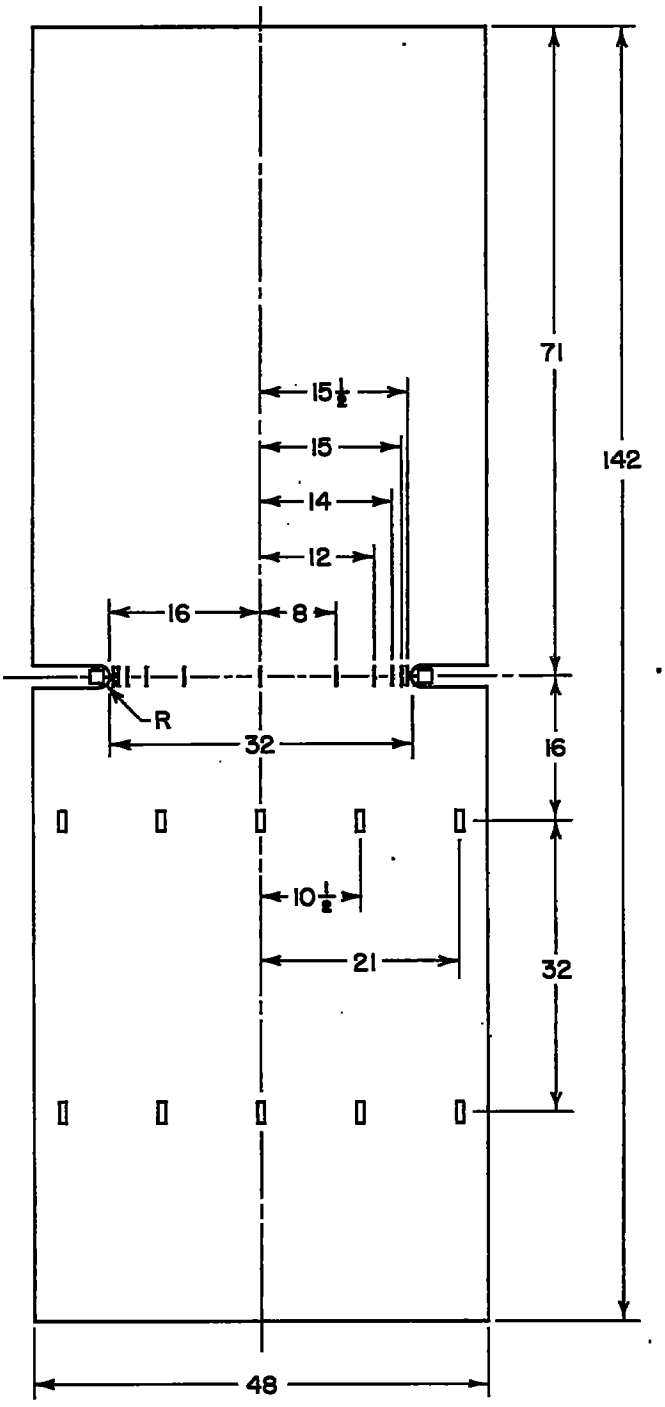

□ Tuckerman gage or electromagnetic gage

▯ SR-4 type A-1 gage

| SR-4 type A-5 gage

Note: Same gaging on opposite side

Panel	R, in.
N2	6.750
N4	1.187
N6	.484

Figure 1.- Dimensions and instrumentation of notched specimens. (All dimensions are in inches.)

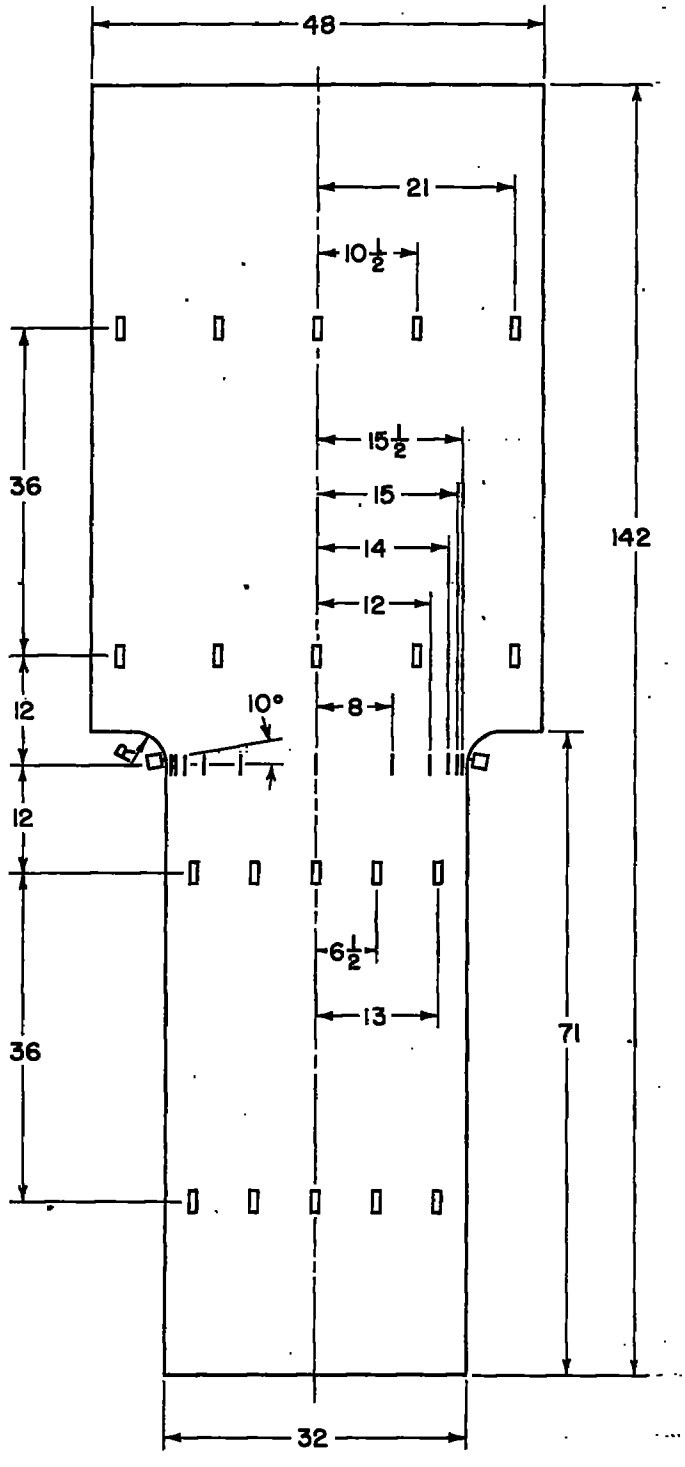

Tuckerman gage or electromagnetic gage

SR-4 type A-1 gage

SR-4 type A-5 gage

Note: Same gaging on opposite side

Panel	R, in.
F2	3.703
F4	.656
F6	.266

NACA

Figure 2.- Dimensions and instrumentation of filleted specimens. (All dimensions are in inches.)

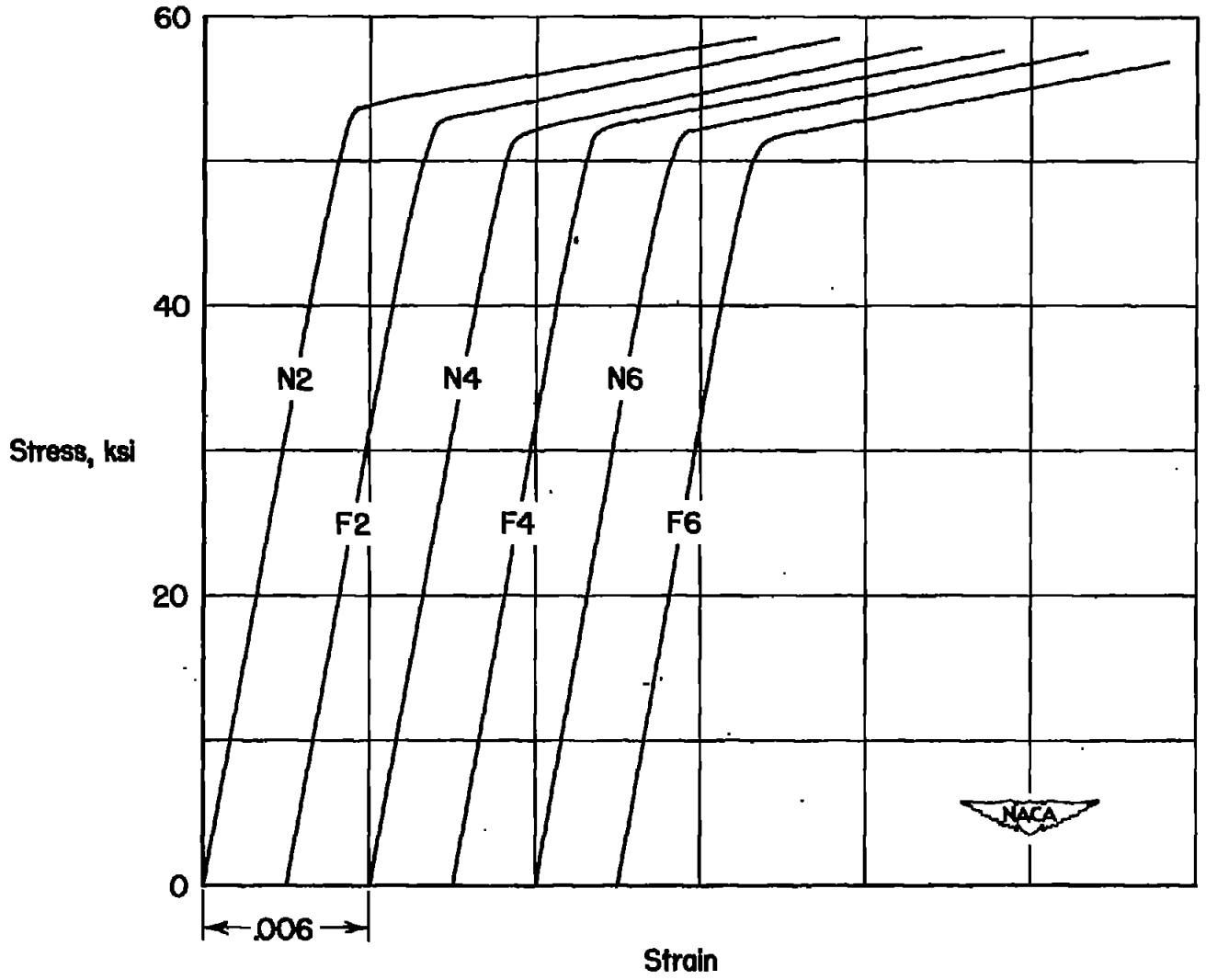

Figure 3.- Stress-strain curves of 24S-T3 aluminum alloy for each specimen tested.

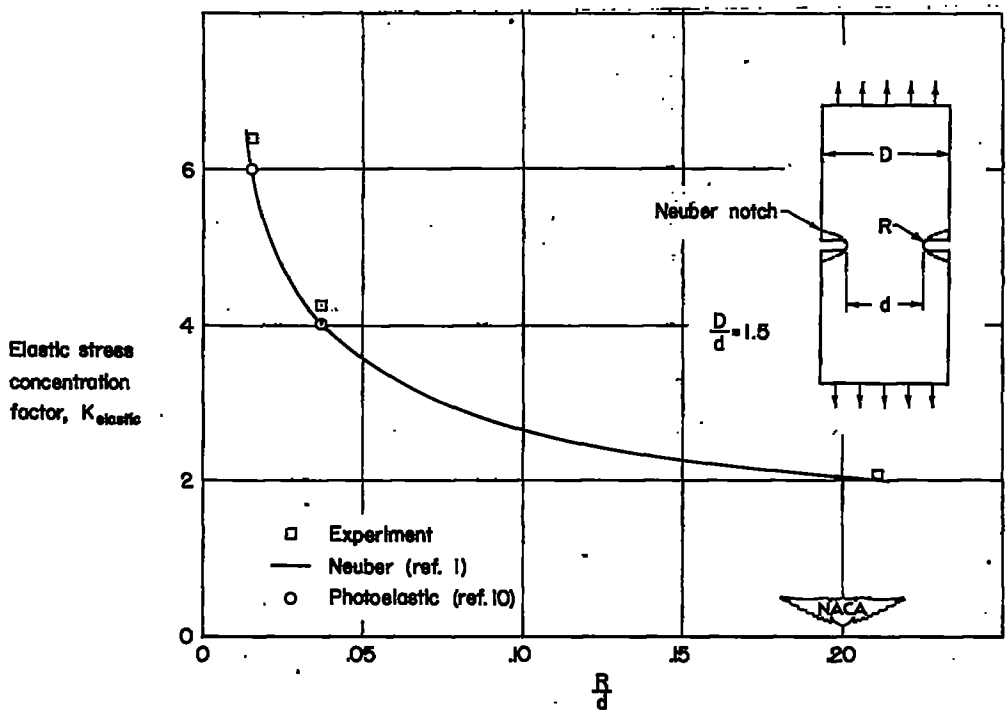

Figure 4.- Elastic stress concentration factors for notched specimens.

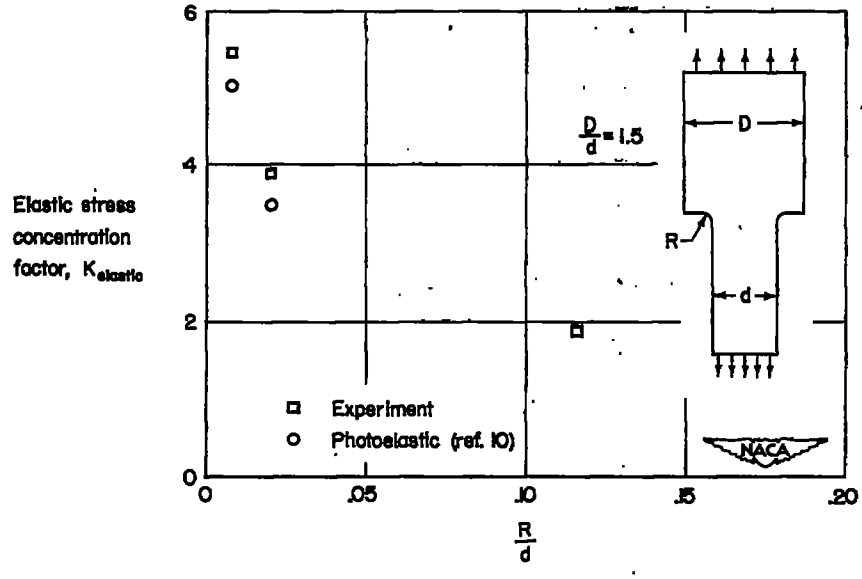

Figure 5.- Elastic stress concentration factors for filleted specimens.

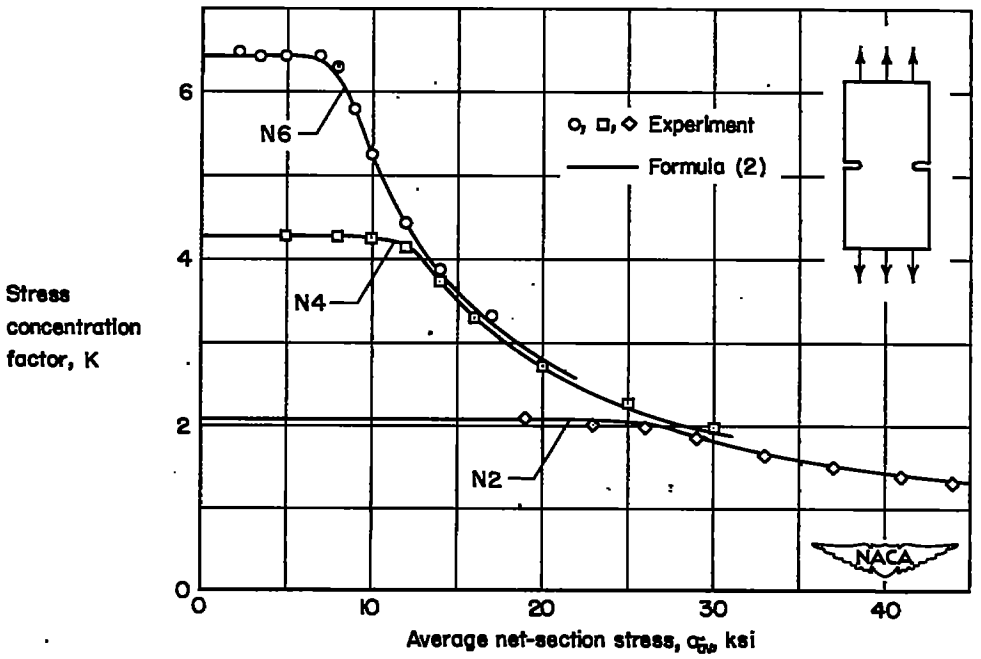

Figure 6.- Stress concentration factors for notched specimens.

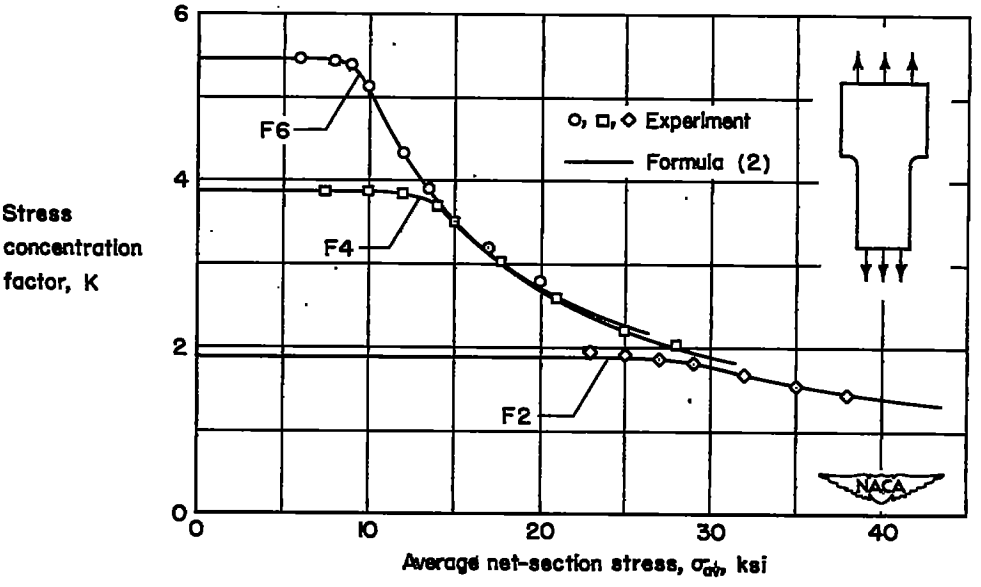

Figure 7.- Stress concentration factors for filleted specimens.

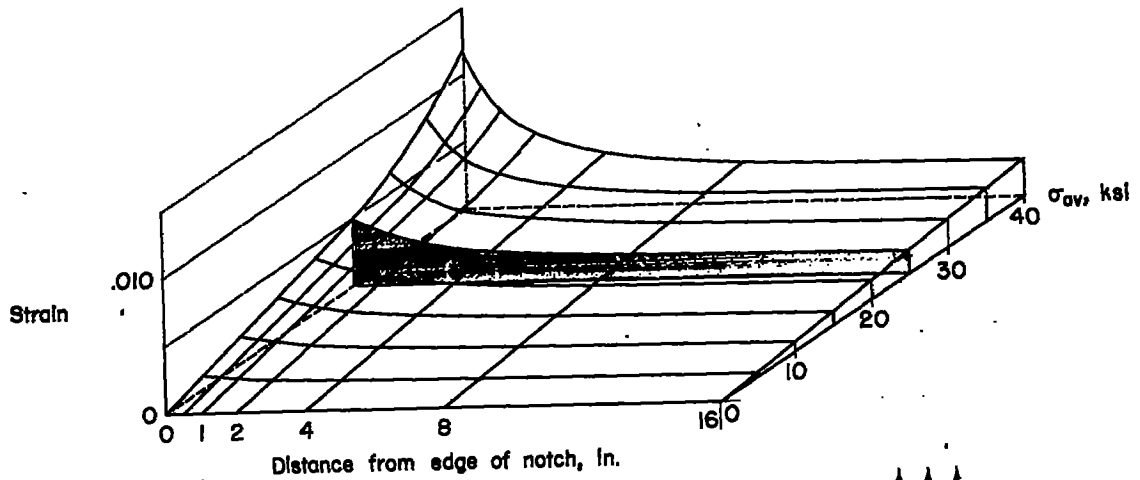

(a) Strain distribution.

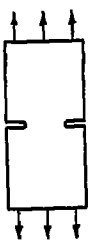

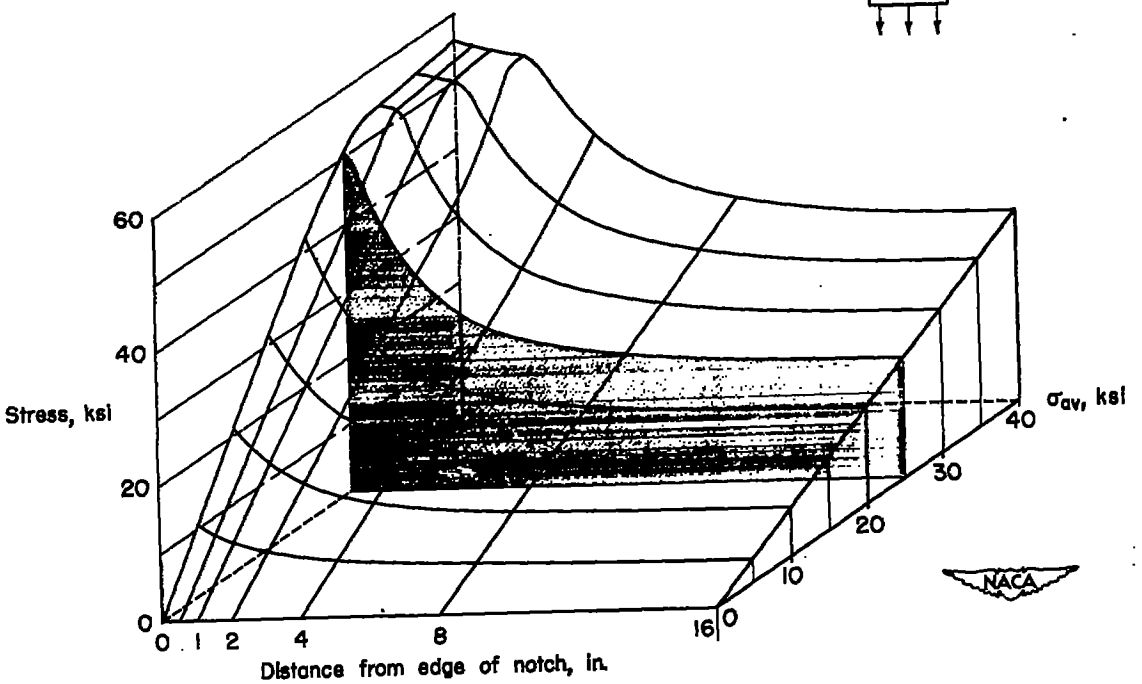

(b) Apparent stress distribution.

Figure 8.- Strain distribution and apparent stress distribution at the net section of specimen N2.

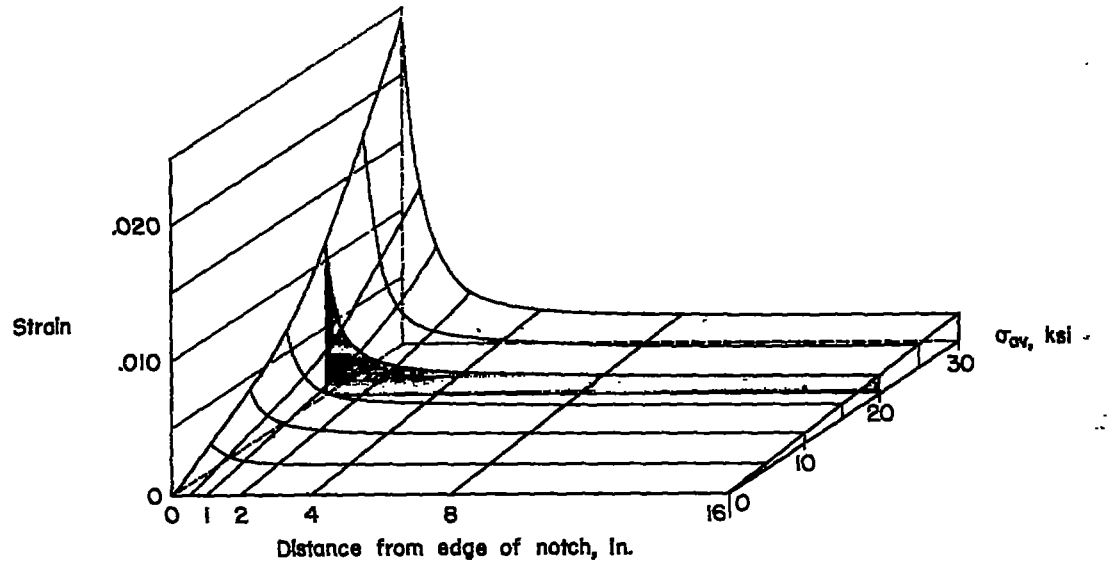

(a) Strain distribution.

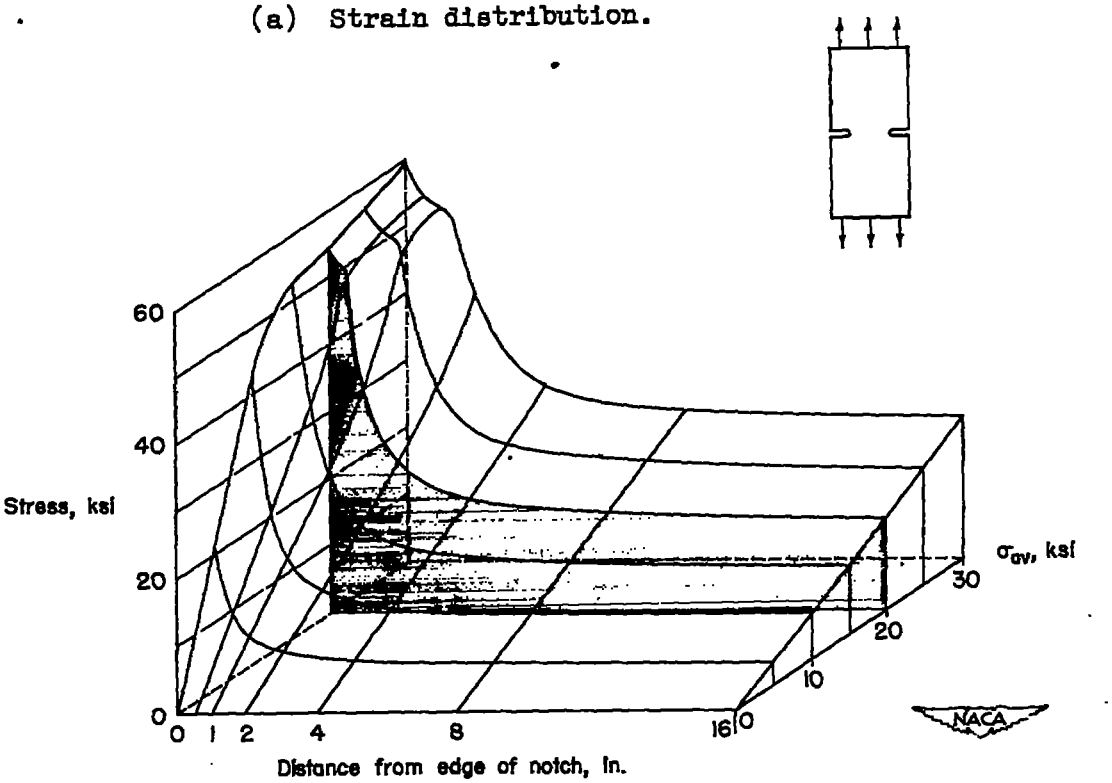

(b) Apparent stress distribution.

Figure 9.- Strain distribution and apparent stress distribution at the net section of specimen N4.

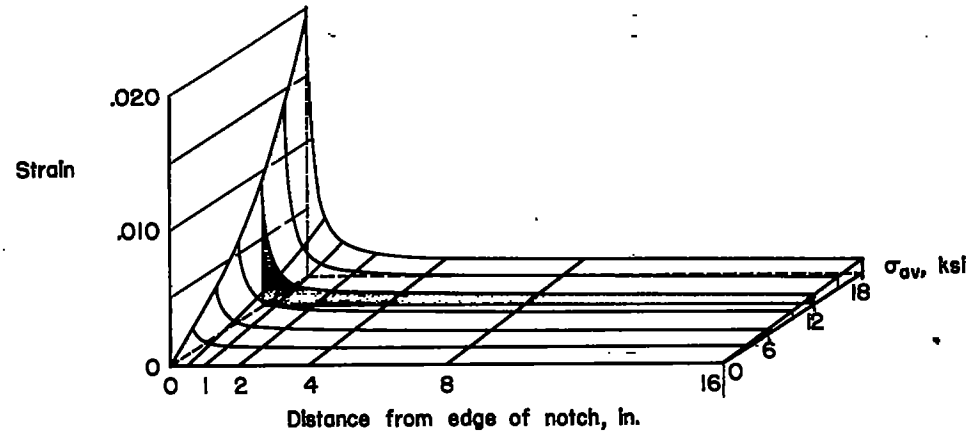

(a) Strain distribution.

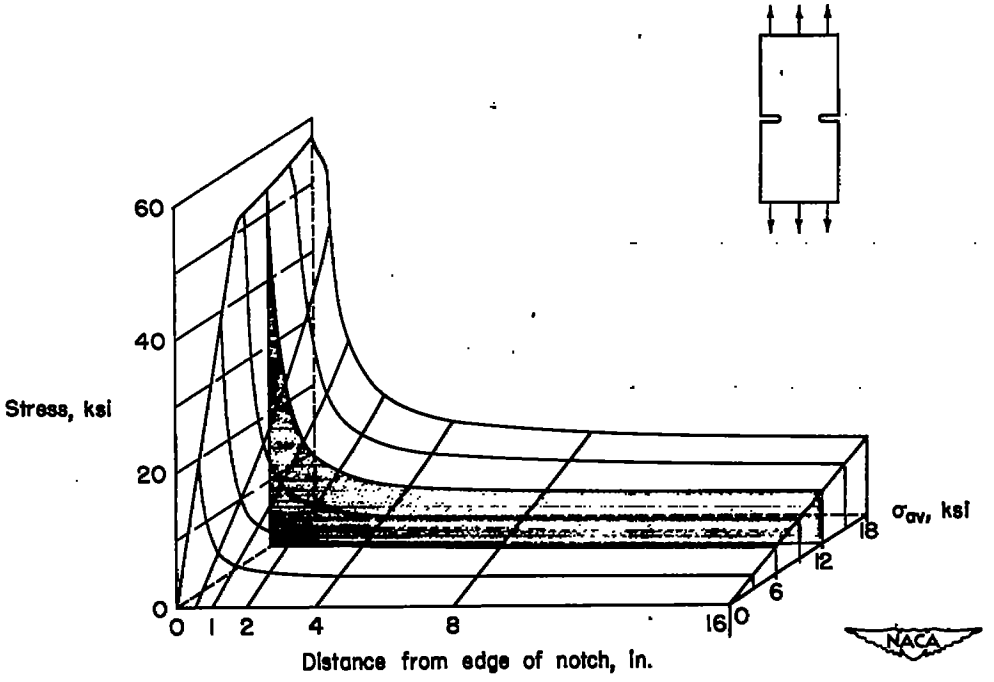

(b) Apparent stress distribution.

Figure 10.- Strain distribution and apparent stress distribution at the net section of specimen N6.

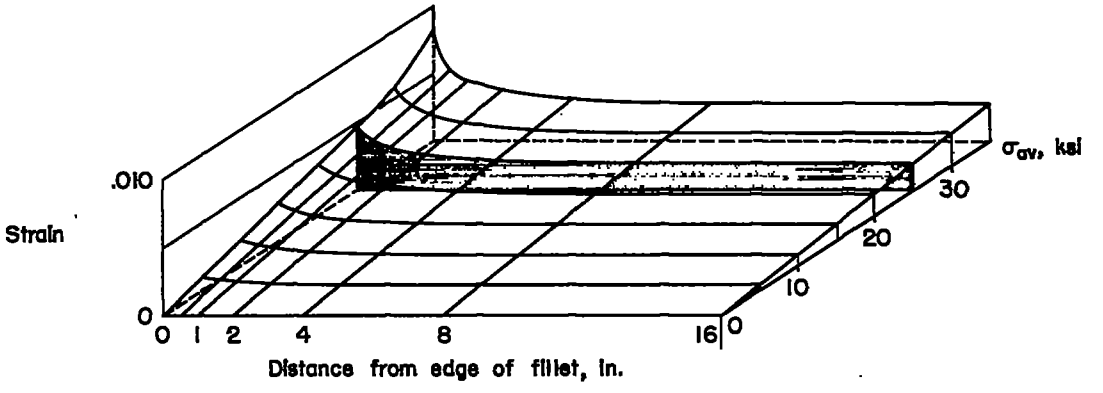

(a) Strain distribution.

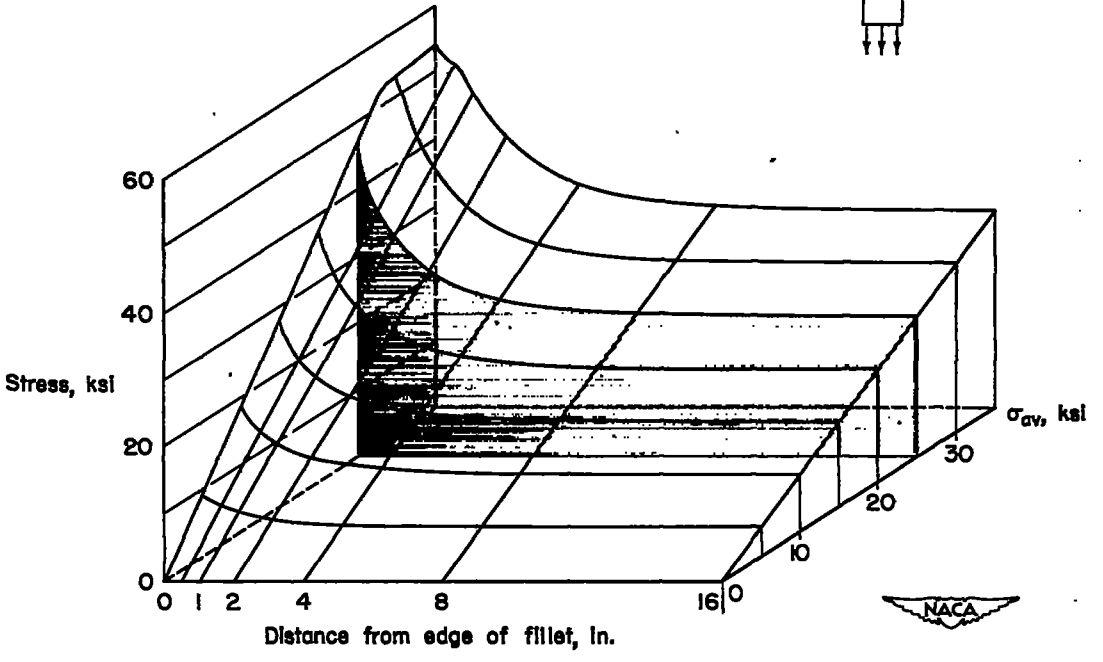

(b) Apparent stress distribution.

Figure 11.- Strain distribution and apparent stress distribution at the net section of specimen F2.

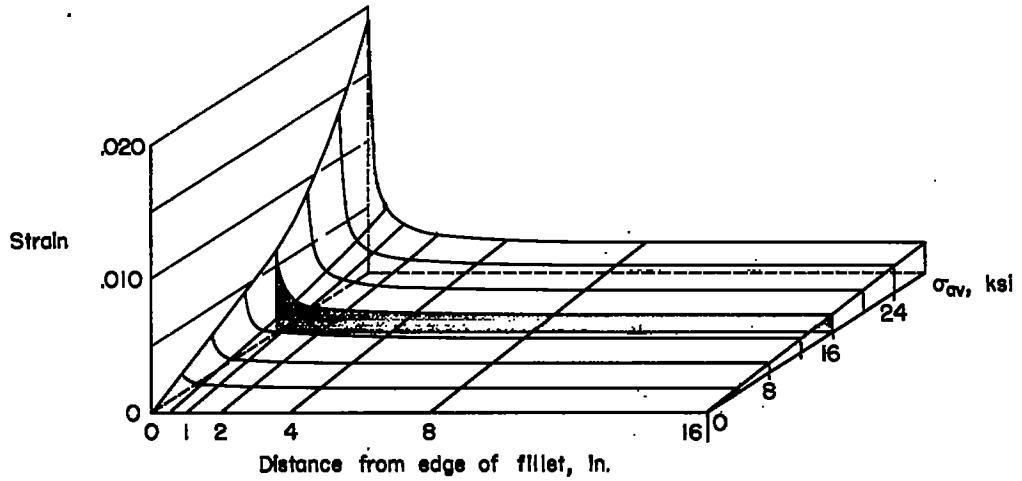

(a) Strain distribution.

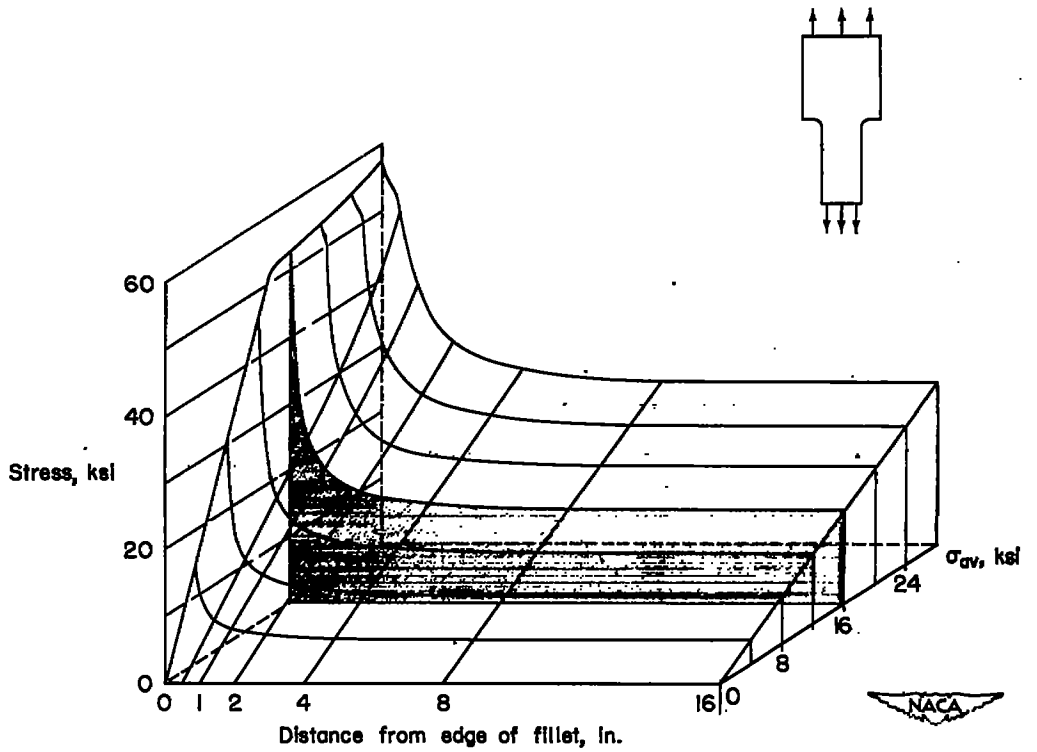

(b) Apparent stress distribution.

Figure 12.- Strain distribution and apparent stress distribution at the net section of specimen F4.

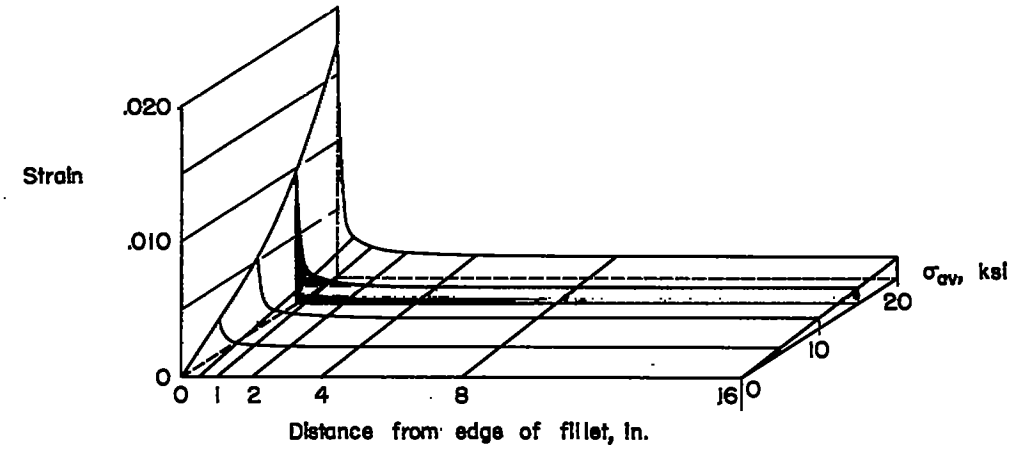

(a) Strain distribution.

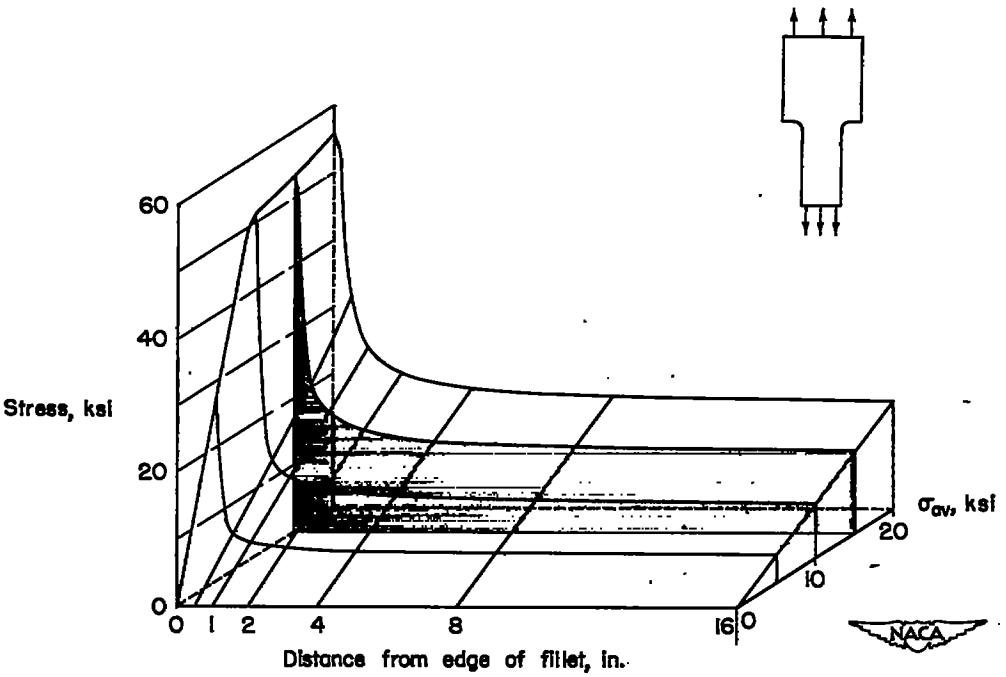

(b) Apparent stress distribution.

Figure 13.- Strain distribution and apparent stress distribution at the net section of specimen F6.

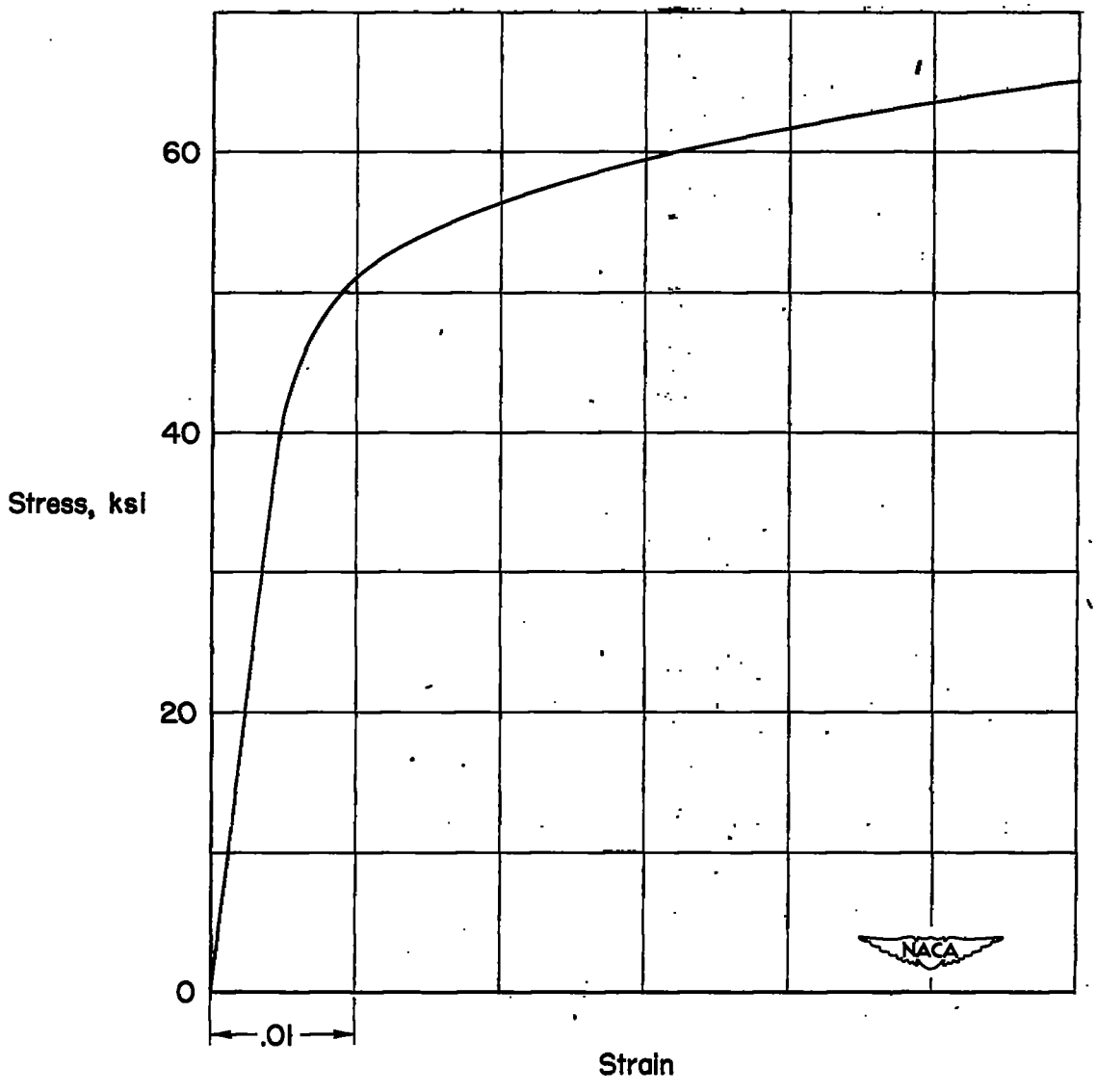

Figure 14.- Stress-strain curve for 24S-T3 aluminum alloy used in reference 9.

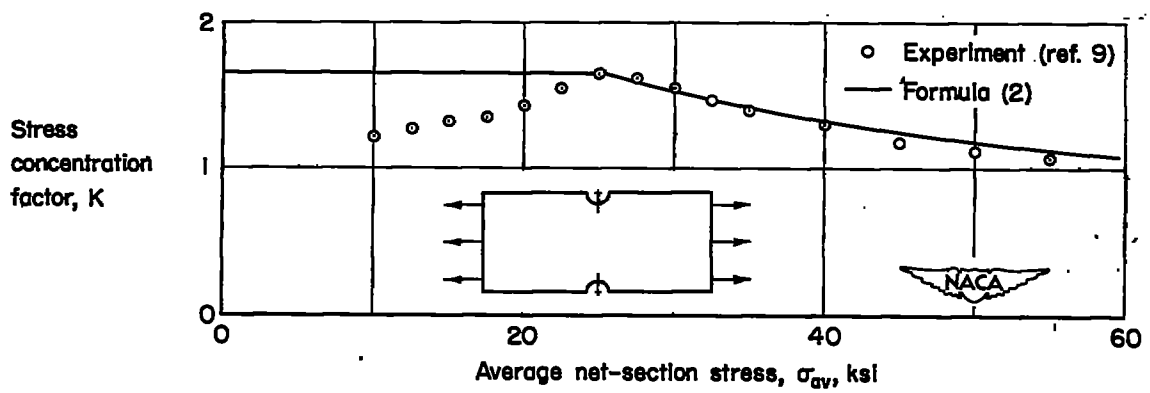

Figure 15.- Stress concentration factor for a flat plate with semicircular edge notches.

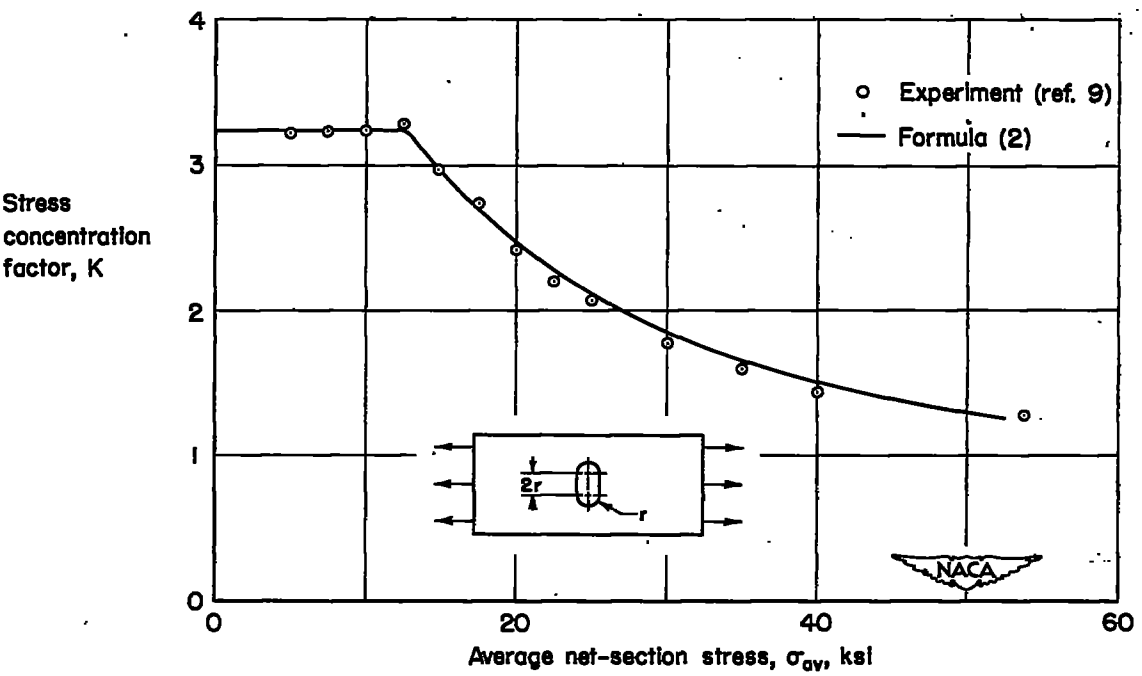

Figure 16.- Stress concentration factor for a flat plate with a single central hole elongated in the transverse direction.

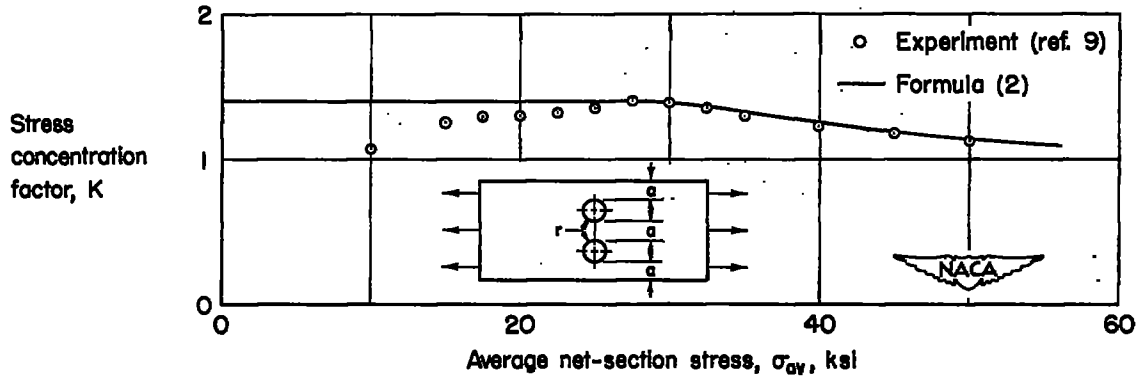

Figure 17.- Stress concentration factor for a flat plate with two circular holes equally spaced in one cross section.

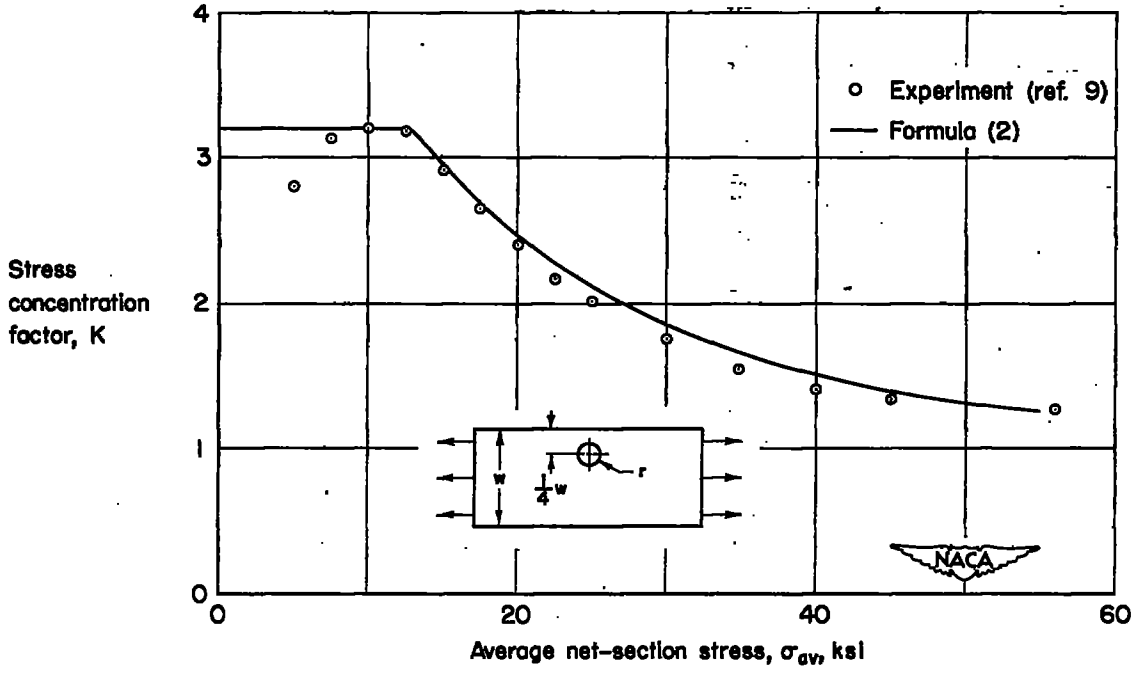

Figure 18.- Stress concentration factor for a flat plate with a circular hole located $\frac{1}{4}$w from the edge.

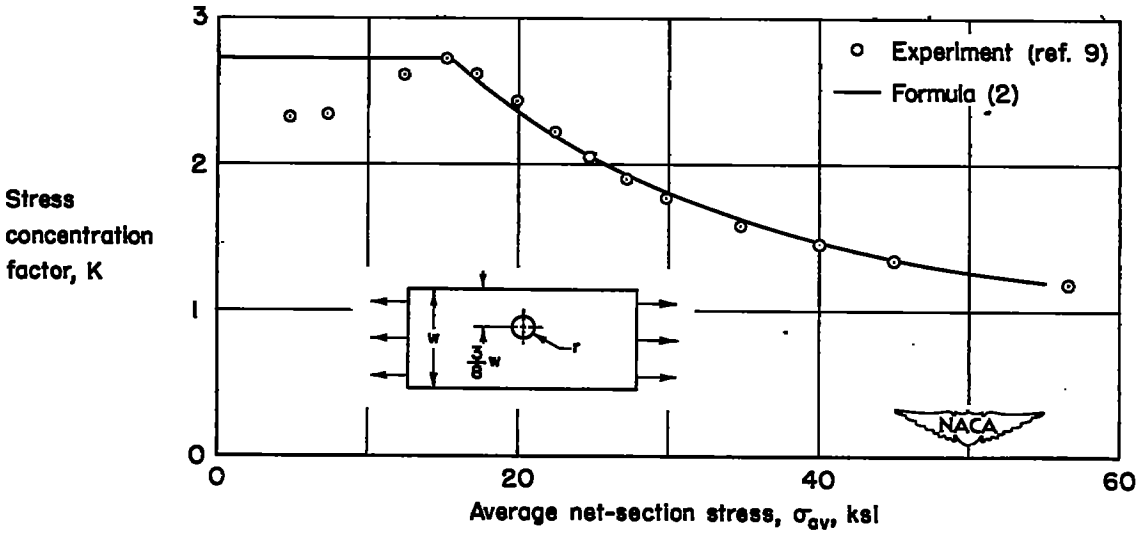

Figure 19.- Stress concentration factor for a flat plate with a circular hole located $\frac{3}{8}w$ from the edge.

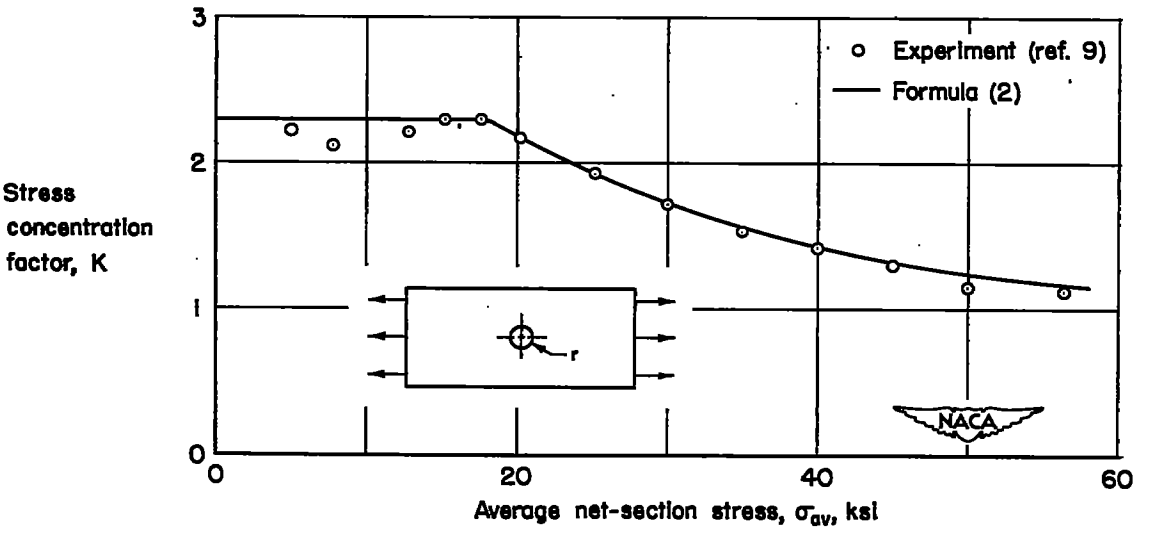

Figure 20.- Stress concentration factor for a flat plate with a single, central, circular hole.

NACA-Langley - 12-3-51 - 1000